

Magnetization and peak effect of several single crystals of V_3Si

M. Isino,* T. Kobayashi,† N. Toyota, T. Fukase, and Y. Muto
Institute for Materials Research, Tohoku University, Sendai 980, Japan

(Received 15 December 1987)

Magnetization is measured on several $A15$ V_3Si single crystals. The magnetization curve of the purest sample, which is a high- κ superconductor in the pure limit, is fairly reversible, accompanied by an upward curvature near H_{c2} probably caused by the Pauli paramagnetic effect. Those of the other samples show the peak effect near H_{c2} , and a scaling law between the pinning force density F_p and the magnetic field holds. The magnetic induction B changes nonlinearly across the sample, and the sign of d^2B/dr^2 changes at the field where F_p attains a maximum. The strain also shows the peak effect near H_{c2} , corresponding closely to that of the pinning force.

I. INTRODUCTION

$A15$ superconductors such as V_3Si and Nb_3Sn have been studied extensively.¹ One of the most interesting subjects is still to clarify the relationship² between a high T_c and lattice instability, the latter of which is often manifested in the low-temperature cubic-to-tetragonal transformation, the so-called martensitic transition.

These two $A15$ compounds have provided a unique opportunity to study the high-field type-II superconductivity in the pure limit ($l \gg \xi_{GL}$; l the electron mean free path and ξ_{GL} the Ginzburg-Landau coherence length). This is ascribed to the fact that both V_3Si ($T_c \cong 17$ K, $H_{c2} \cong 200$ kOe) and Nb_3Sn ($T_c \cong 18$ K, $H_{c2} \cong 250$ kOe) are stoichiometric compounds, which are exceptional in high- T_c $A15$ superconductors. In fact, a number of specific-heat data for the stoichiometric single-crystal V_3Si are reported³⁻⁵ in order to clarify the thermodynamic properties in the type-II superconductivity with high T_c and high H_{c2} in the pure regime. However, their magnetization, especially of single crystals, has not necessarily been studied intensively because of experimental difficulties such as the existence of large hysteresis. For $A15$ superconductors only several data on the magnetization have been reported as follows: Nb_3Sn polycrystalline tubes,⁶ Nb_3Sn single crystals⁷ just below T_c , V_3Ga polycrystalline tubes⁸ near H_{c1} , and V_3Si single crystals^{9,10} near H_{c1} . Even for high- κ superconductors in the dirty limit which have been studied extensively, reversible magnetization curves have been measured only by Hake.¹¹

In this paper we study the magnetization and the strain of several V_3Si single crystals with different purity to investigate the thermodynamic properties and the pinning phenomena.

II. EXPERIMENTAL

Several V_3Si single crystals were prepared by the radio-frequency or electron-beam floating-zone method,¹² and have been used for other measurements such as ultrasonic attenuation and velocity,¹³ specific heat,^{3,14} and

thermal expansion.¹⁵⁻¹⁷ Some of their properties are compiled in Table I, where \mathcal{R} is a ratio of the resistance at room temperature to that just above T_c .

The samples are rectangular prisms with faces of $\{001\}$ and/or $\{011\}$, except sample 1 which has upper and lower faces of $\{001\}$ and an irregular side face. Some samples were annealed at 1300 °C for about 10 h. The annealed sample 4, called 4a, was prepared in order to investigate the annealing effect on the fluxoid pinning. After annealing, this sample was planed in order to remove a few small grains grown on the surface and then chemically etched.

Magnetization was measured in sweeping magnetic field by a method similar to that developed by Ward.¹⁸ A sample was attached to a copper sample holder with Apiezon-N grease. A pair of search coils was wound coaxially and connected so as to compensate the magnetic field. It was displaced by a synchronous motor at 10 rpm between a bottom position surrounding the sample and a top one. The induced signal was integrated by a flux meter, MF-3 from O.S. Walker, Inc. The signal amplified by a home-made preamplifier was reversed simultaneously whenever a pair of search coils come up to the top position. The integrated signal was plotted against the magnetic field with an X - Y recorder at the end of each cycle. A home-made sequence controller was used to operate the reset of the integrator, the reversal of the signal and the pen up and down. A magnetic field up to 80 kOe was generated by a superconducting solenoid. Its magnitude was estimated from the supplied current and its homogeneity was of 5×10^{-4} over a range of the coil displacement. The sweep rate is 3.3 or 6.6 Oe/sec below a few kOe and 33 or 66 Oe/sec above it. The strain was measured by the capacitance dilatometer used in Ref. 10.

Experimental errors were caused mainly by the drift in an electronic system and by both inhomogeneity and hysteresis of the magnetic field generated by the superconducting solenoid. The hysteretic behavior of the solenoid which was evident up to 20 kOe decreases with increasing magnetic field. Because of the drift in our electronic system, the magnetization curves were normalized by assuming that the susceptibility in the normal state χ_N is an average of the measured values at different temperatures

TABLE I. Characterization and properties of V₃Si single crystals.

	Sample number				
	1	4	4a	5	7-2
Cross-section area (mm ²)	~34	2.94×3.37	2.68×2.86	5.18×5.34 5.16×5.18	5.97×9.10
Height (mm)	7.5	7.00	6.88	5.16 5.34	4.49
Side faces	irregular	(100)	(100)	(110) (100) (110)	(110)
Upper and lower faces	(001)	(001)	(001)	(001) (011)	(001)
\mathcal{R}	17-12	10	10	90	10
Demagnetizing factor	0.35±15%	0.29±2%	0.24±2%	0.47±4% 0.47±4%	0.6±10%
T_c (K)	16.7	16.4	16.4	16.9	16.4
$-(dH_{c2}/dT)_{T_c}$ (kOe/K)	22.9	24.0	23.5		21.4
h_p	0.75~0.85	0.86	0.88		0.85
n	4.0	3.3	3.0		4.3

though χ_N is known to depend strongly on temperature.¹⁹ The values of χ_N thus obtained are 4.5, 5.9, and 6.6×10^{-5} emu/cm³±30% for samples 5, 1, and 4, respectively.

The temperature of the sample holder was measured at $H=0$ by a calibrated germanium resistance thermometer and was kept constant within 0.03 K in sweeping field by a capacitance temperature controller. The sample was heated always above 35 K before each sweep to set the sample in a magnetically virgin state ($T > T_c = 16.4 \sim 17$ K) and also in a high-temperature cubic phase ($T > T_m \cong 20-27$ K) for the transforming samples. Sometimes it was heated only just above T_c ; there were no differences in the magnetization curves between these two cases.

Demagnetizing factors of samples 4 and 5 were determined from the magnetization curves in the Meissner state of vanadium samples with a size similar to those two samples. Vanadium was chosen as a reference material because it has high H_{c1} . The demagnetizing factors of samples 1 and 7-2 were assumed appropriately from a slope of the magnetization curve in the Meissner state.

The magnetization curves of almost all type-II superconductors show hysteresis more or less. In the model of Fietz and Webb,²⁰ both the equilibrium magnetization M_e and the critical current density J_c can be obtained from the magnetization curves in increasing and decreasing fields for a cylindrical sample, if higher-order terms can be neglected. The model assumes that (1) the sample is in the critical state, (2) the surface current is negligible, and (3) the flux density B changes continuously across the sample. We applied the model to a sample with a rectangular cross section by assuming that J_c flows parallel to the surface.²¹ Then,

$$4\pi(M_+ + M_-) = 2(4\pi M_e) - (4\pi/c)2C_2 J'_c \quad (1)$$

and

$$4\pi(M_+ - M_-) = (4\pi/c)2C_1 J_c, \quad (2)$$

where M_+ and M_- is the magnetization in increasing and decreasing field, respectively, $J_c = dB/dr$ and $J'_c = d^2B/dr^2$, and r is a direction perpendicular to the surface. The constants C_1 and C_2 are

$$[b^2/6 + (a-b)b/4]/a$$

and

$$[b^3/48 + (a-b)b^2/24]/a,$$

respectively, where a and b are the length of the longer and shorter side of the rectangular cross section. Higher-order terms not shown explicitly in Eqs. (1) and (2) are neglected in our analysis.

III. RESULTS AND DISCUSSIONS

A. Magnetization of high- κ superconductor in the pure limit

The magnetization curve of the purest sample 5 with $\mathcal{R}=90$, is fairly reversible except both near H_{c1} and just below H_{c2} . The hysteresis becomes prominent with decreasing temperature. Figure 1 shows the magnetization curve at 12.54 K in increasing and decreasing field, for example. In sample 1 whose resistance ratio \mathcal{R} is 17, the mean free path is estimated to be twice as long as the coherence length.³ Since \mathcal{R} of sample 5 is 90, we conclude that sample 5 with $l \cong 10\xi_{GL}$ is a high- κ superconductor in the pure limit. Therefore the magnetization curves of sample 5 provide the most reliable data for the equilibrium magnetization of high- κ superconductors in the pure limit (κ , Ginzburg-Landau parameter).

Figure 2 shows both H_{c2} and H_p in magnetic field along [001] and [011] directions; the magnetic field H_p where the magnetic flux begins to penetrate into the sample should be regarded as an upper limit of H_{c1} .

The values of H_{c2} when the field is applied along the [001] and [011] directions agree with each other within experimental errors, and $(dH_{c2}/dT)_{T_c} = -14.0$ kOe/K. Resistivity measurements by Kramer and Knap²² and

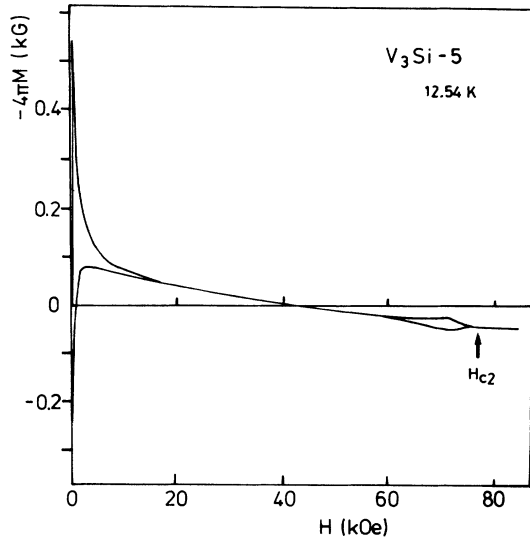


FIG. 1. The magnetization curve of the sample 5 single-crystal V_3Si at 12.54 K. H_{c2} is defined by the arrow.

Foner and McNiff²³ show that the anisotropy of H_{c2} is about 2%. The discrepancy in these data, however, may result from the uncertainty in determining H_{c2} from the magnetization curves of samples where large hysteresis appears near H_{c2} . The parabolic law of H_p shown by the solid line in Fig. 2 as the upper limit of H_{c1} agrees roughly with the data of Eckert and Berthel.¹⁰

The equilibrium magnetization M_e is estimated by assuming that it is an average of the magnetization in increasing and decreasing fields and that it changes smoothly just above H_p . It was also assumed that M_e changes linearly in an irreversible region below H_{c2} . Figure 3 shows M_e curves thus obtained for the magnetic field applied along the [001] direction, where the solid

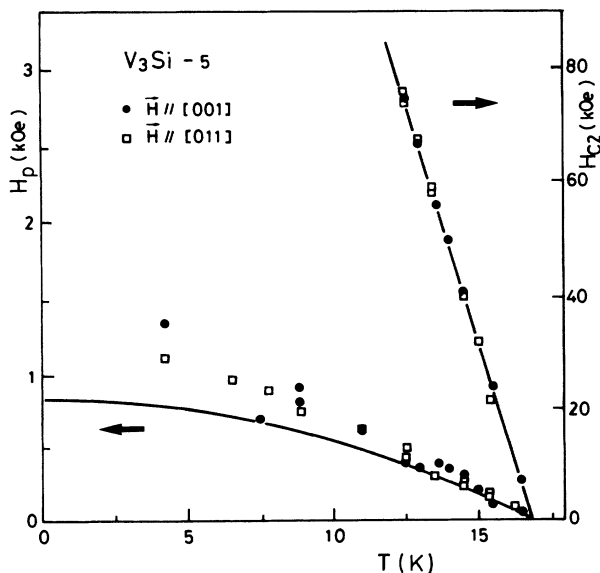


FIG. 2. The temperature dependence of H_{c2} and H_p in $H \parallel [001]$ and $\parallel [011]$ for sample 5. H_p in Ref. 10 is also included.

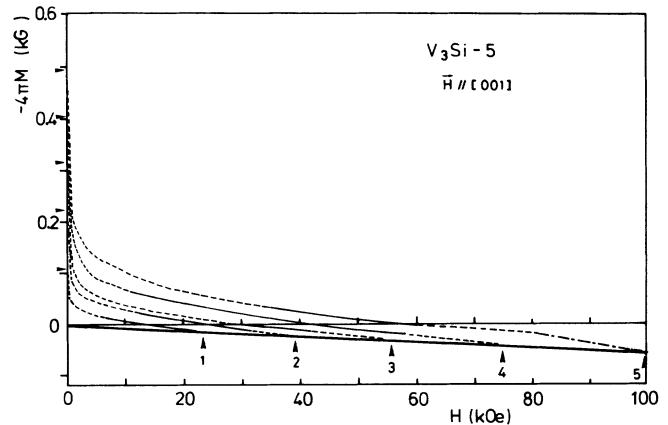


FIG. 3. Analyzed magnetization curves at (1) 15.50 K, (2) 14.53 K, (3) 13.52 K, (4) 12.54 K, and (5) 11.01 K for sample 5 in $H \parallel [001]$. The solid curve for the observed reversible curve, the dashed curve for the mean value of the hysteresis magnetization, and the dash-dotted curve (only for the 11.01 K data with the estimated $H_{c2} \cong 100$ kOe) for the extrapolated curve of the dashed one below 80 kOe.

line is the observed curve in the reversible region and the dashed line is the mean value of $(M_+ + M_-)/2$. The dot-dashed region at 11.01 K is an extrapolated one up to H_{c2} ($\cong 100$ kOe) which is estimated from the extrapolation in the H_{c2} curve in Fig. 2. It should be noted that the linearity of M_e of a high- κ superconductor in the pure limit is observed only near H_{c2} with decreasing field from H_{c2} , whereas the magnetization of a high- κ superconductor in the dirty limit is linear from H_{c2} down to rather near H_{c1} . It is also clear that the M_e curve becomes non-linear near H_{c2} more and more with decreasing temperature.

Figure 4 shows both thermodynamic critical field H_c

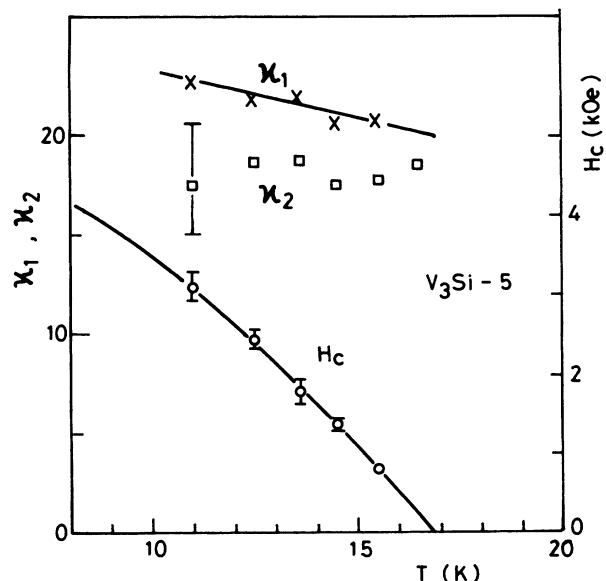


FIG. 4. The temperature dependence of the thermodynamic critical field H_c and the Ginzburg-Landau parameters of κ_1 and κ_2 .

obtained from the M_e curves and Ginzburg-Landau parameters κ_1 , κ_2 , and κ . These three parameters are obtained by the following equations:

$$\kappa_1 = \frac{H_{c2}}{\sqrt{2}H_c}, \quad (3)$$

$$-4\pi M_e = \frac{H_{c2} - H}{(2\kappa_2^2 - 1)\beta_A}, \quad (4)$$

and

$$\kappa = \frac{1}{\sqrt{2}} \frac{(dH_{c2}/dT)_{T_c}}{(dH_c/dT)_{T_c}}, \quad (5)$$

where H is the external magnetic field and β_A is the Abrikosov parameter of 1.16. Experimental errors in κ_2 are large since M_e is analyzed from a magnetization curve obtained by using Eqs. (1) and (2). Then κ is estimated to be 20 ± 2 from the data of H_c and H_{c2} . The magnitude of κ is a little larger than the intrinsic GL parameter 16.8 estimated from the specific-heat data³ of sample 1.

According to the theory of Maki and Tsuzuki,²⁴ κ_2 is expected to increase with decreasing temperature and to be larger than κ_1 in low- κ type-II superconductors in the pure limit,²⁴ κ_2 of the purest V_3Si is roughly independent of temperature, while κ_1 increases with decreasing temperature.

It should be noted in Fig. 3 that the magnetization M_e shows an upward curvature near H_{c2} which is often observed in high- κ superconductors in the dirty limit.¹¹ The magnetic behaviors of high- κ superconductors in the dirty limit^{25,26} are different from that of low- κ superconductors in the dirty limit. The Pauli paramagnetic effect reduces the superconducting condensation energy and results in a first-order transition to the normal state at a relatively low field compared with H_{c2}^* which is determined only by the orbital effect. On the other hand, the spin-orbit coupling tends for the spin angular momentum to be uncertain so as to diminish and cancel the Pauli paramagnetic effect. In real superconductors where both effects work simultaneously, an intermediate behavior appears. For example, the magnetization curve of Ti-16 at. % Mo (Ref. 11) shows an upward curvature near H_{c2} similar to that of sample 5, and both κ_1 and κ_2 decrease with decreasing temperature. No theoretical prediction is reported on the Pauli paramagnetic effect of type-II superconductivity in the pure limit and no data to be compared is available on high- κ superconductors in the pure limit. Our data suggest the importance of the Pauli paramagnetic effect in pure V_3Si . This suggestion was previously pointed out by Orlando *et al.*²⁷ from the results of H_{c2} in a V_3Si thin film.

B. Peak effect in the magnetization and the strain

A peak of the magnetization near H_{c2} is prominent in samples other than the purest sample 5. Figure 5 shows magnetization curves of sample 4. The hysteresis of this sample is larger than that of sample 5 as expected from the smaller $\mathcal{R} = 10$. The peak near H_{c2} becomes pronounced with decrease in temperature.

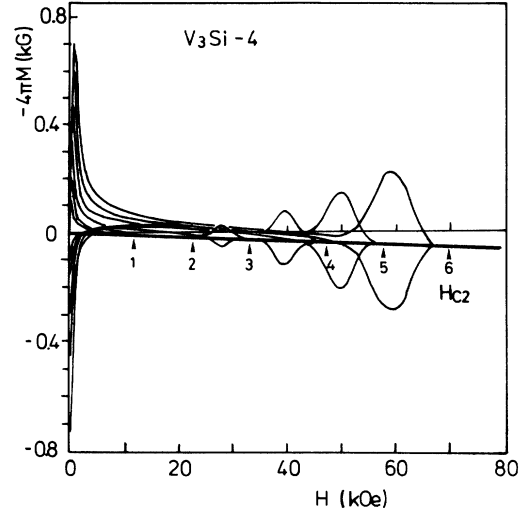


FIG. 5. Magnetization curves of sample 4 at several temperatures: (1) 15.85 K, (2) 15.55 K, (3) 15.04 K, (4) 14.50 K, (5) 14.01 K, and (6) 13.55 K. H_{c2} is defined by the arrow.

In many superconducting materials the critical current decreases to a minimum with increasing field and then recovers to some maximum before it falls to zero at H_{c2} ; this phenomenon is the so-called "peak effect." Campbell and Evetts²⁸ summarized experimental data of the peak effect and classified those into two types, a broad peak at intermediate fields and a narrow peak just below H_{c2} . The peak observed in V_3Si belongs to the latter, which is thought to be related to the rigidity of the fluxoid line lattice.²⁹

Figure 6 shows the pinning force density $F_p = J_c H$ of sample 4, where J_c is derived from the magnetization curves by using Eq. (2). Figure 7 plots F_p/F_p^{\max} (F_p^{\max} is the maximum value of F_p) of sample 4 against the reduced field $h (= H/H_{c2})$ at several temperatures. The overlap of F_p^{\max} curves indicates clearly that a universal

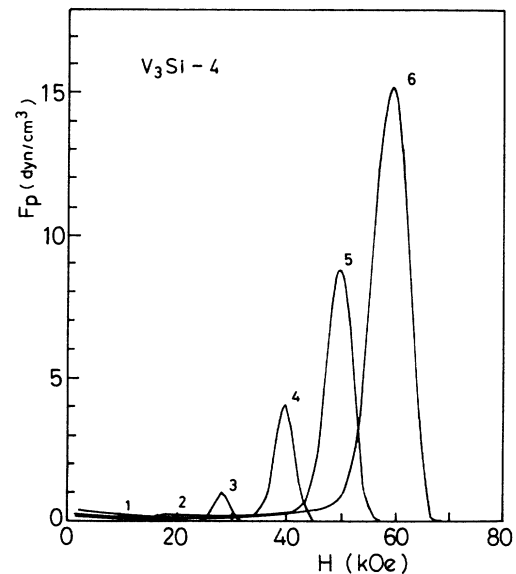


FIG. 6. Pinning force density F_p as a function of the applied field H for sample 4.

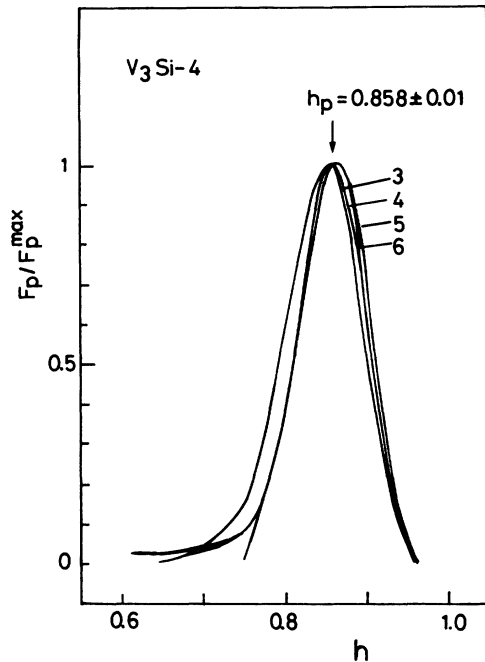


FIG. 7. The pinning force density normalized by the maximum one, F_p/F_p^{\max} , as a function of the reduced field $h=H/H_{c2}$.

function exists and the reduced field h_p at which F_p takes a maximum is 0.86. Thus, a scaling law of the following form,

$$F_p = H_{c2}^n f(h), \quad (6)$$

holds as observed previously for a variety of materials,^{30,31} where f is a function of h and n is a material constant.

A scaling law also holds both for the annealed sample 4a, where J_c flows in the $\langle 001 \rangle$ direction as in sample 4 and for sample 7-2 with $\mathcal{R}=10$, where J_c flows in the $\langle 011 \rangle$ direction, and $f(h)$ of sample 7-2 is similar to that shown in Fig. 7. On the other hand, it does not hold for sample 1 with $\mathcal{R}=17$, where J_c flows along irregular surface, and h_p increases with decreasing temperature up to 0.85 at 13.4 K, as observed similarly in Nb-50 at. % Ta alloy.³² It is concluded that a scaling law for the peak effect holds in samples of $\mathcal{R} \leq 10$.

Even the purest sample 5 with $\mathcal{R}=90$ among the V_3Si samples has a small peak around h_p , which increases with decreasing temperature. In samples 1 and 4 where the density of pins is higher than that of sample 5 a large peak appears around $h_p=0.75-0.85$, which increases with decreasing temperature, as observed in Nb-Ta.³² The scaling law holds at low temperatures where h_p becomes constant.

The values of h_p and n are listed in Table I. All the values of h_p of V_3Si single crystals are around 0.85, and the form of $f(h)$ is similar. The obtained values of n for our single crystals exhibiting the peak effect scatters between 3.0 and 4.3.

Although the obtained values of n scatter somewhat, the peak effect in V_3Si should be caused by the same pin-

ning mechanism because the values of h_p are almost constant and the shapes of $f(h)$ are similar to each other. The data of Osborne and Kramer³³ on Nb-Ta alloys show that h_p is rather constant with increase in the density of pins till the peak effect vanishes.

The magnitude of n in ordinary hard superconductors is confined between 2 and 3 (Refs. 30 and 31) but, in the presence of the peak effect, the values between 2.9 and 4.6 have been reported,^{32,34-38} as supported also by our data. Though Pulver³⁷ and Alekseevskii *et al.*³⁸ show that the pinning effect of V_3Si single crystals are extremely anisotropic, the values of n in V_3Si also scatter in the same range as those of the peak effect in isotropic superconductors.

The critical current in V_3Si single crystals has been measured by Pulver³⁷ and Alekseevskii *et al.*³⁸ They observed a peak effect of J_c at $h_p=0.87$ (Ref. 37) and 0.9 (Ref. 38); the latter is a little higher than the former probably because H_{c2} determined by the linear extrapolation in the J_c versus H curve is a little lower than the real H_{c2} . Therefore, the value of h_p of our sample agrees with their values. It has also been observed that the peak effect does not necessarily appear in all the crystallographic directions even in the same sample.³⁷ A scaling law similar to that found in our samples seems to hold in their samples. In the case where J_c flows in the $\langle 001 \rangle$ direction in magnetic field, n is 4.0 and 4.2 for the samples of Pulver³⁷ and Alekseevskii *et al.*,³⁸ respectively, and these values are larger than those of our samples. In another case where J_c flows in the $\langle 110 \rangle$ direction, the value of 4.3 for sample 7-2 is much larger than 2.3 of Pulver when the field is applied along $\langle 001 \rangle$ direction. The sample of Pulver does not show the peak effect and is guessed to have a high density of pins. A peak effect with $h_p=0.87$ is also observed in the radio-frequency loss of V_3Si single crystals,³⁹ but the direction along which J_c flows is not described.

Pulver³⁷ and Alekseevskii *et al.*³⁸ observed a remarkable anisotropy of J_c , but its origin has not yet been made clear. It is well known that the lattice properties such as Young's modulus⁴⁰ are highly anisotropic, and this may enhance the anisotropy of J_c . On the other hand, both groups observed different anisotropy of J_c in their measurements when J_c flows in the $\langle 110 \rangle$ direction. This shows that the arrangement of pins which are effective when J_c flows in the $\langle 110 \rangle$ direction is sensitively dependent on the sample preparation. In other words, the anisotropy of J_c is probably ascribable not to the anisotropy of lattice properties but to plane pins. Planar defects in the $A15$ -type superconductor, however, were not well investigated. Only subboundaries caused by the pile up of dislocations in V_3Si (Ref. 41) and stacking faults in Nb_3Sn (Ref. 42) were reported as their origins. Pulver's data when J_c flows in the $\langle 110 \rangle$ direction (Fig. 4 of Ref. 37) suggest that plane pins exist also in planes of low symmetry though such planar defects have not yet been reported. Then, it is guessed that our samples also have plane pins.

It is not always valid in the model of Fietz and Webb to neglect higher-order terms in order to obtain the equi-

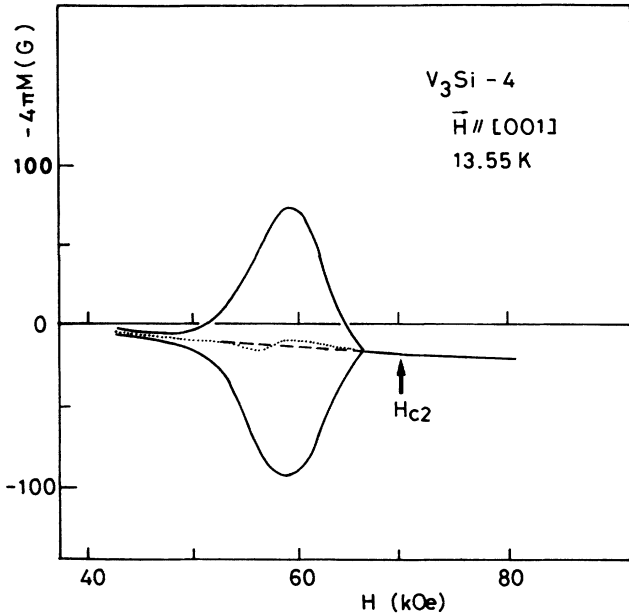


FIG. 8. Detailed magnetization curve at 13.55 K near H_{c2} of sample 4 demonstrating the peak effect.

librium magnetization. Figure 8 shows the magnetization curve of sample 4 around the peak. A dotted line indicates the average of the magnetization with increasing and decreasing fields. Kartascheff⁴³ suggested that the equilibrium magnetization of niobium which shows the peak effect changes nonlinearly just like the dotted line. However, his experimental procedure does not eliminate a possibility for the nonequilibrium current to flow around the sample, and his suggestion is not correct. If we assume the equilibrium magnetization changes linearly as shown by the dashed line, we can obtain d^2B/dr^2 from Eq. (1).

Figure 9 shows dB/dr and d^2B/dr^2 as a function of H for sample 4. The value of d^2B/dr^2 is of the same order of magnitude of dB/dr and changes its sign near h_p . This suggests an alternative pinning mechanism at h_p as

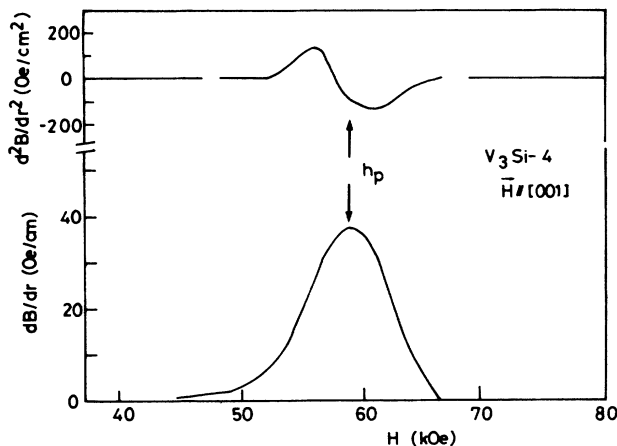


FIG. 9. The magnetic field dependence of the first and second derivatives of the induction B with the coordinate r in the plane normal to H , for sample 4 and $H \parallel [001]$.

suggested, for example, by Kramer.³⁰ An abrupt change in the current-voltage characteristics has already been reported at h_p .^{38,44} Several models have been presented on the peak effect.⁴⁵ For example, Kramer³⁰ suggested for line pins that F_p change as $b^2(1-b)$ above h_p and as $b/(1-b)$ below it, where b is the reduced flux density. This b dependence of F_p is consistent with the change in the sign of d^2B/dr^2 .

C. Strain

A peak effect is also observed in the longitudinal magnetostriction¹⁵ of sample 1, which is measured by both methods A and B as described below. In method A the strain is measured at the center of the sample, while in method B an average of the strain over the sample is measured by placing a copper plate onto the sample. The former is more appropriate than the latter because the pinning force causes the strain to vary over the sample. Figure 10 shows a hysteretic behavior of the strain at 15.0 K obtained by method A when the applied field is parallel to the $\langle 001 \rangle$ direction. A pronounced peak appears around h_p in increasing and decreasing fields corresponding to the peak in the magnetization. The strain measured by method B also shows a remarkable peak around h_p . When the field is applied in the $\langle 011 \rangle$ direction, the strain is measured only by method B . In this case the strain changes in a complicated manner around h_p , and this may be due to the strain inhomogeneity over the sample.

The strain of V_3Si in the mixed state changes linearly and is much larger than that of ordinary superconductors. The martensitic transformation of V_3Si which starts just above T_c is arrested at T_c by the appearance of superconductivity before the complete growth of the transformation.² Since the strain above H_{c2} continues smoothly to the strain extrapolated from above T_c , the large linear change in the mixed state is considered to recover to the value which can be expected if superconductivity does not appear. The orientation of tetragonal domains in V_3Si is so sensitive to the applied stress that the hysteresis of the strain, except around the peak, may be caused by the hysteresis of magnetization and also by a

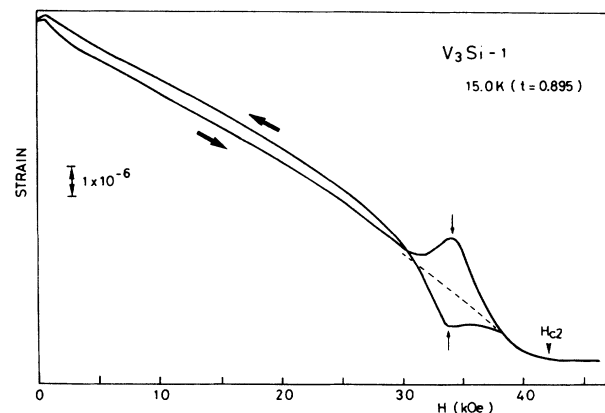


FIG. 10. The strain as a function of increasing and decreasing fields, for sample 1 at 15.0 K. H_{c2} is defined by the arrow.

reorientation of tetragonal domains forces by the pinning force.

If the strain is assumed as the dashed line shown in Fig. 10 when no pinning force is exerted on the sample, the strain due to the pinning force in increasing field can be obtained as shown by the dashed line displayed in Fig. 11. The reversed peak in decreasing field is owing to the reversal of the direction of the pinning force.

Kronmüller⁴⁶ studied theoretically the strain in a homogeneous superconductor. In real superconductors the strain due to the pinning force should be taken into his theory. Then Eq. (31) in Ref. 46 can be extended as follows:

$$\text{div}\sigma^{(t)} + f^{(Q)} + f^{(H)} + f^{(P)} = 0, \quad (7)$$

where $\sigma^{(t)}$ is the strain, $f^{(Q)}$ is the force due to the ground-state energy of a superconductor, $f^{(H)}$ is the force due to the Lorentz force, and $f^{(P)}$ is the pinning force which is newly introduced. In an inhomogeneous superconductor the distribution of the magnetization in a sample cannot be expressed easily. Here, we use the Bean model⁴⁷ that J_c is constant, and neglect the surface current because of large κ . Then near H_{c2} ,

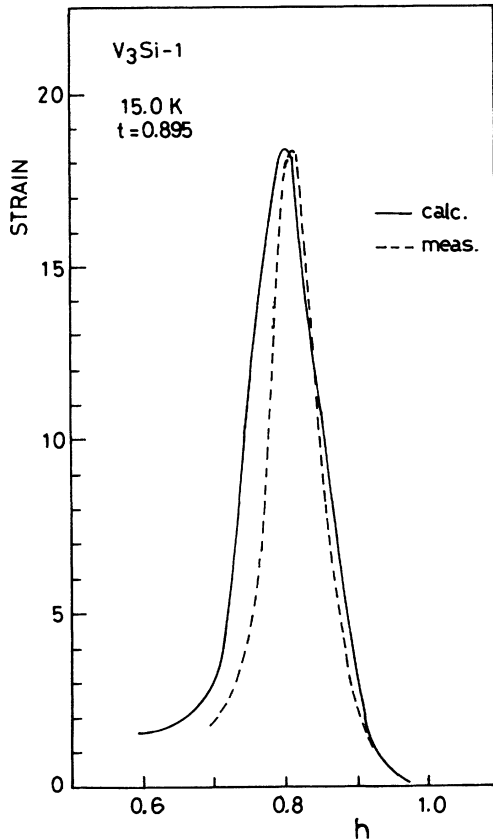


FIG. 11. Comparison of the strain l/l_0 vs reduced field h between the measured curve and the calculated one using the magnetization curve.

$$f_1^{(P)} = f_2^{(P)} = -J_c \left[H_{\text{ext}} \left[\frac{H_{\text{ext}} - H_{c2}}{(2\kappa^2 - 1)\beta_A} \pm \frac{4\pi}{c} J_c (r - R) + \chi H_{\text{ext}} \right] (1 - N_3) \right],$$

and

$$f_3^{(P)} = 0,$$

where the suffixes 1, 2, and 3 of $f^{(P)}$ mean a component of $f^{(P)}$ in the 1, 2, and 3 direction, respectively. H_{ext} is applied along the 3 direction, R is half the distance between the planes counter to each other, r the distance from the center, N_3 the demagnetizing factor in the 3 direction, and \pm the decrease and increase of H_{ext} , respectively.

Then,

$$e_{zz} = \frac{-2C_{11}\sigma_{xx} + (C_{11} + C_{12})\sigma_{zz}}{C_{11}(C_{11} + C_{12}) - 2C_{12}^2}, \quad (8)$$

where e_{zz} is the strain in the 3 direction, σ_{xx} and σ_{zz} are the stress in the 1 and 3 direction, respectively, and C_{11} and C_{12} are the elastic constants in the cubic crystal. At fields near H_p where $\sigma_{xx} \gg \sigma_{zz}$,

$$e_{zz} = \frac{-2C_{12}}{C_{11}(C_{11} + C_{12}) - 2C_{12}^2} \sigma_{xx}. \quad (8')$$

The proportional factor in the right-hand side of Eq. (8') becomes enhanced in $V_3\text{Si}$ near the martensitic transformation temperature where $C_{11} \cong C_{12}$.

If we take C_{11} to be 1.7×10^{12} dyn/cm² and the elastic shear modulus C_s [$= (C_{11} - C_{12})/2$] to be 0.024×10^{12} dyn/cm² reasonably, a solid line displayed in Fig. 11 can be calculated from the measured value of the pinning force. The solid line is very similar to the dashed line (experimental data). This clearly proves that the peak effect in strain is caused by the peak effect in the pinning force.

To summarize, the magnetization of the purest sample 5 $V_3\text{Si}$ single crystal is fairly reversible and its upward curvature near H_{c2} is ascribable to the Pauli paramagnetic effect. Other low-quality single crystals exhibit pronounced peak effect near H_{c2} ($h=0.85$) and obey a scaling law for the pinning force density. The magnetic induction changes nonlinearly across the sample. The sign of d^2B/dr^2 changes at the field h_p where F_p attains a maximum and this suggests a change in the dominant pinning mechanism at h_p . A peak effect observed in the magnetostriction is revealed to reflect the peak effect of the flux pinning phenomena.

In this paper, we could not clarify in detail the effect of the tetragonal domains induced by the martensitic transformation on the superconducting mixed state in $V_3\text{Si}$. This problem may be quite complicated and is open to further studies.

- *Present address: Aoyama Patent Office, 2-10 Honmachi Higashiku, Osaka, Japan.
- †Present address: ANELVA Corporation, 8-1 Yotsuya 5-chome Fuchu-shi, Tokyo 183, Japan.
- ¹For recent reviews, J. Muller, Rep. Prog. Phys. **43**, 641 (1980); and S. V. Yu. Vonsovsky, A. Izyumov, and E. Z. Kurmaev, *Superconductivity of Transition Metals* (Springer-Verlag, New York, 1982).
- ²M. Kataoka and N. Toyota, Phase Trans. **8**, 157 (1987); N. Toyota, B (to be published); N. Toyota, T. Kobayashi, M. Kataoka, H. F. J. Watanabe, T. Fukase, Y. Muto and H. Takei, J. Phys. Soc. Jpn., No. 9 (1988).
- ³Y. Muto, N. Toyota, K. Noto, K. Akutsu, M. Isino, and T. Fukase, J. Low Temp. Phys. **34**, 617 (1979).
- ⁴C. C. Huang, A. M. Goldman, and L. E. Toth, Solid State Commun. **33**, 581 (1980).
- ⁵A. Junod and J. Muller, Solid State Commun. **36**, 721 (1980).
- ⁶Y. B. Kim, C. F. Hempstead, and A. R. Strunad, Phys. Rev. **129**, 528 (1963).
- ⁷J. J. Hanak, J. J. Halloran, and G. D. Cody, *Proceedings of the Tenth International Conference on Low Temperature Physics, Moscow, 1966*, edited by P. Malkov, L. P. Pitaevski, and A. Shal'nikov (VINITI, Moscow, 1967), Vol. II A, p. 373.
- ⁸D. L. Decher and H. L. Laquer, J. Appl. Phys. **40**, 2817 (1969).
- ⁹R. Brand and W. W. Webb, Solid State Commun. **7**, 19 (1969).
- ¹⁰D. Eckert and K. H. Berthel, Cryogenics **15**, 479 (1975).
- ¹¹R. R. Hake, Phys. Rev. **158**, 356 (1967).
- ¹²S. Ono, I. Haryu, N. Toyota, and T. Fukase, Tech. Rep. (RIISOM) **8**, 79 (1978) (in Japanese).
- ¹³N. Toyota, T. Fukase, M. Tachiki, and Y. Muto, Phys. Rev. B **21**, 1827 (1980).
- ¹⁴K. Akutsu, K. Noto, T. Fukase, N. Toyota, and Y. Muto, J. Phys. Soc. Jpn. **41**, 1431 (1976).
- ¹⁵T. Fukase, T. Kobayashi, M. Isino, N. Toyota, and Y. Muto, J. Phys. (Paris) Colloq. **39**, C6-406 (1978).
- ¹⁶T. Kobayashi, T. Fukase, N. Toyota, and Y. Muto, Physica **107B**, 261 (1981).
- ¹⁷T. Kobayashi, T. Fukase, N. Toyota, and Y. Muto, in *Superconductivity in d- and f-Band Metals*, edited by W. Buchel and W. Weber (Kernforschungszentrum, Karlsruhe, 1982). p. 59.
- ¹⁸D. Ward, Cryogenics **7**, 41 (1967).
- ¹⁹W. E. Blumberg, J. Eisinger, V. Jaccarino, and B. T. Matthias, Phys. Rev. Lett. **5**, 149 (1960).
- ²⁰W. A. Fietz and W. W. Webb, Phys. Rev. **178**, 657 (1969).
- ²¹We have neglected the details of the distribution of current shown by A. Shadowitz, Phys. Rev. B **23**, 3250 (1981).
- ²²E. J. Kramer and G. S. Knapp, J. Appl. Phys. **46**, 4595 (1975).
- ²³S. Foner and E. J. McNiff, Jr., Phys. Lett. **58A**, 318 (1976).
- ²⁴K. Maki and T. Tsuzuki, Phys. Rev. **139**, A868 (1965).
- ²⁵N. R. Werthamer, E. Helfand, and P. C. Hohenberg, Phys. Rev. **147**, 295 (1966).
- ²⁶K. Maki, Phys. Rev. **148**, 362 (1966).
- ²⁷T. P. Orlando, E. J. McNiff, Jr., S. Foner, and M. R. Beasley, Phys. Rev. B **19**, 4545 (1979).
- ²⁸A. M. Campbell and J. E. Evetts, Adv. Phys. **21**, 327 (1972).
- ²⁹E. J. Kramer, J. Nucl. Mater. **72**, 5 (1978).
- ³⁰E. J. Kramer, J. Appl. Phys. **44**, 1360 (1973).
- ³¹D. Dew-Hughes, Philos. Mag. **30**, 293 (1974).
- ³²K. E. Osborne, Philos. Mag. **23**, 1113 (1971).
- ³³K. E. Osborne and E. J. Kramer, Philos. Mag. **29**, 685 (1974).
- ³⁴D. M. Kroeger, Solid State Commun. **7**, 843 (1969).
- ³⁵M. S. Kroeger and D. M. Kroeger, Physica **55**, 394 (1971).
- ³⁶S. Borka, I. N. Goncharov, D. Fricsovszky, and I. S. Khukhareva, Fiz. Nizk. Temp. **3**, 716 (1977) [Sov. J. Low Temp. Phys. **3**, 347 (1977)].
- ³⁷M. Pulver, Z. Phys. **257**, 22 (1972).
- ³⁸N. E. Alekseevskii, N. M. Dobrovolskii, A. V. Dubrovik, E. P. Krasnoperov, and V. A. Marchenko, Fiz. Tverd. Tela (Leningrad) **17**, 2065 (1975) [Sov. Phys.—Solid State **17**, 1349 (1976)].
- ³⁹E. P. Krasnoperov and P. A. Chemnykh, Fiz. Tverd. Tela (Leningrad) **22**, 2112 (1980) [Sov. Phys.—Solid State **22**, 1230 (1980)].
- ⁴⁰L. R. Testardi and T. B. Bateman, Phys. Rev. **154**, 402 (1967).
- ⁴¹Y. Uzel and H. Diepers, Z. Phys. **258**, 126 (1973).
- ⁴²H. J. Levinstein, E. S. Greiner, and H. Mason, Jr., J. Appl. Phys. **57**, 164 (1966).
- ⁴³N. Kartascheff, J. Low Temp. Phys. **21**, 203 (1975).
- ⁴⁴B. D. Lauterwasser and E. J. Kramer, Phys. Lett. **53A**, 410 (1975).
- ⁴⁵J. R. Patel and B. W. Battermann, J. Appl. Phys. **37**, 3447 (1966).
- ⁴⁶H. Kronmüller, Phys. Status Solidi **40**, 295 (1970).
- ⁴⁷D. Eckert and A. Handstein, Phys. Status Solidi A **37**, 171 (1976).